

Laplacian growth in self-consistent Laplacian field : Effect of the long-range interparticle interactions on the fractal dimension of structures formed by their aggregation-limited diffusion.

F. Carlier, E. Brion, and V. M. Akulin

Laboratoire Aimé Cotton, Bât. 505, CNRS II, Campus d'Orsay, Orsay Cedex F-91405, France

We numerically simulate the dynamics of aggregation of interacting atomic clusters deposited on a surface. We show that the shape of the structures resulting from their aggregation-limited random walk is affected by the presence of a binary interparticle Laplacian potential due to, for instance, the surface stress field. We characterize the morphologies we obtain by their Hausdorff fractal dimension as well as the so-called external fractal dimension, which appears more sensitive to the potential. We demonstrate the relevance of our model by comparing it to previously published experimental results for antimony and silver clusters deposited onto graphite surface.

I. FREE AND BIASED DIFFUSION MODELS

Highly ramified dendritic structures often appear in nature in such different situations as cell colony growth [1], dielectric breakdown [2], viscous fingering in Hele-Shaw cells [3], liquid crystal growth [4], electro-deposition [5], single-atom [6, 7] and atomic cluster depositions [8–11]. Though the objects observed are not mathematically rigorous fractals, the self-similarity they show on a certain range of the probe length justifies the (strictly speaking improper) use of this term to qualify them [12].

The description common to all these systems relies on the diffusion equation

$$\partial_t P(t, \vec{r}) = D \Delta P(t, \vec{r}) \quad (1)$$

written for the probability distribution $P(t, \vec{r})$ and completed by the conditions imposed on the gradient $\vec{\nabla} P(t, \vec{r} \in \partial S)$ at the boundaries ∂S of the area S occupied by the structure at a given moment of time t . In the quasistatic regime, when a typical time of boundary variations always remains much longer than SD^{-1} , the probability satisfy the Laplace equation $\Delta P(t, \vec{r}) = 0$ with the boundary conditions [13] evolving as the structure grows. This regime allows an elegant description based on conformal mapping, which accounts for the structure dynamics [3, 14].

An alternative description relies on random walk models, including the widely known Diffusion Limited Aggregation (DLA) model [15], which yields a good visual agreement with experimentally observed morphologies [8]. The models are based on a probabilistic dynamical process

$$\vec{r}_i(t) \xrightarrow{p(\vec{r}_i, \vec{r}'_i)} \vec{r}'_i(t + \Delta t) \quad (2)$$

according to which the i -th particle located at a point \vec{r}_i jumps into the point \vec{r}'_i within the step $t \rightarrow (t + \Delta t)$ with the probability $p(\vec{r}_i, \vec{r}'_i) = p(\vec{r}'_i, \vec{r}_i)$. This process is assumed to last until the particle touches another particle and stops, thus contributing to an immobile aggregated dendrite. A link between those two approaches was identified in [16], giving rise to hybrid methods such

as the iteration of random conformal mappings [17–19] which generate DLA-type objects.

Still the results of experiments with atomic clusters deposited at a surface and aggregated to dendritic structures in the course of diffusion, are just in a qualitative agreement with the DLA simulations [20], whereas careful inspection reveals discrepancies in compactness of the experimental and the DLA-induced structure, thus indicating that some physical ingredients are missing in the model. In the present work, we assume that the missing element is a Laplacian field induced by the aggregated clusters and acting onto the moving ones. The Laplacian field can be of different origins, and one of the options is a surface stress field, which results from the mismatch of the crystalline structures of the cluster and the substrate material and yields mutual attraction of the deposited clusters. In this new setting, the actual motion of clusters is no longer a free but a biased random walk with asymmetric jumping probabilities $p(\vec{r}_i, \vec{r}'_i, t) \neq p(\vec{r}'_i, \vec{r}_i, t)$, which on average can be described by the well-known Smoluchowski equation for the probability distribution

$$\partial_t P(t, \vec{r}) = \left(\vec{f}(t, \vec{r}) \cdot \vec{\nabla} \right) P(t, \vec{r}) + D(t, \vec{r}) \Delta P(t, \vec{r}), \quad (3)$$

where the drift force term $\vec{f}(t, \vec{r})$ and the diffusion coefficient $D(t, \vec{r})$ are respectively the first and second moments of the transition probabilities p .

The numerical simulation of the resulting “drifted” DLA model yields pictures that are in a better agreement with experimental results. One can go beyond this subjective visual estimate and employ the fractal dimension as a quantitative characteristic of the dendritic forms considered which allows for a meaningful and objective comparison between the model and the experiments. We show that, even though the Hausdorff-Minkowski dimension may be used for our purpose, the so-called external fractal dimension is much more adapted due to its great sensitivity to the intensity of the stress field. Confronting our model to experimental results thanks to this tool, we find excellent agreement for antimony-cluster structures. Our model, however, suggests that a repulsive force is at work in the case of silver clusters, which is incompatible with an elastic field.

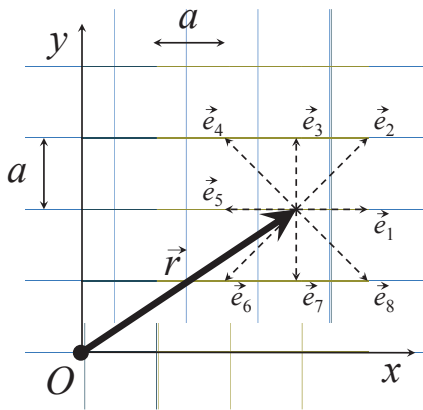


Figure 1: The square lattice in the eight-connectivity model: each site is characterized by its position vector \vec{r} and connected to its eight neighbours $(\vec{r} + \vec{e}_i)_{i=1,\dots,8}$.

The paper is structured as follows. In Sec. II, we present the drifted DLA model in detail, provide simulations and discuss the influence of the stress field on the morphologies obtained as well as their visual agreement with experimentally observed structures. Sec. III is devoted to the characterization of the ramified structures obtained, either experimentally or numerically, through their fractal dimension. In Sec. IV, this quantitative tool is used to discuss the agreement between our model and some experimental results published in the literature. We conclude in Sec. V and suggest some possible perspectives of our work.

II. THE BIASED RANDOM WALK MODEL AND THE EMERGING SHAPES OF CLUSTER AGGREGATIONS

We start by presenting some technical details of the numerical approach employed for the cluster aggregation modelling and the results of simulations follow. The surface of the substrate is considered as a two-dimensional square lattice of step a . Each site can store one cluster at most, and its position is characterized by a vector \vec{r} (see Fig. 1).

At the beginning of a deposition experiment, a first cluster is dropped onto the surface and diffuses freely on the substrate. At each time step of its random walk, this cluster can thus jump from the site \vec{r} it occupies to one of its eight closest neighbours of respective positions

$(\vec{r} + \vec{e}_i)$, with the same (isotropic) probability $p_{iso} = \frac{1}{8}$. At some point of its diffusive exploration of the surface, this cluster reaches a default of the substrate where it stops. The corresponding site is arbitrarily chosen as the origin O of the coordinates – its position vector is therefore $\vec{s}_1 = \vec{0}$. This first cluster is now ready to play the role of a seed for a ramified fractal-like structure.

A second cluster is then dropped onto the surface at a random site – not “too far” from the origin, otherwise it would take it too long to reach the seed by diffusion, and diffuses on the substrate now subject to the force implied by the interaction with the first cluster fixed at the origin. Assuming this force is proportional to the elastic deformation of the substrate and therefore scales like $1/r$ according to Hooke’s law [21], it can be viewed as deriving from the inter-cluster interaction potential $v(r) = \alpha \ln(r/r_0)$, where the length parameter r_0 and the energy parameter α characterize the potential range and intensity, respectively. The relevant force $\vec{F}(\vec{r}) = -\vec{\nabla}_{\vec{r}}v(\vec{r}) = -\alpha\vec{r}/r^2$ acting on the moving cluster affects the transition probabilities which now take the form

$$p(\vec{r}, \vec{r} + \vec{e}_i) \simeq \frac{1}{8} - \frac{\beta}{\|\vec{e}_i\|} \left(\vec{F}(\vec{r}) \cdot \vec{e}_i \right), \quad (4)$$

with $\beta = 1/k_B T$, as it follows from the Smoluchowski equation. For this expression to be valid, the anisotropic term $-\beta\vec{F}_1(\vec{r}) \cdot \frac{\vec{e}_i}{\|\vec{e}_i\|}$ must remain small compared to the isotropic probability $p_{iso} = \frac{1}{8}$, which ensures that the cluster motion never reaches the ballistic regime but keeps its diffusive character. The second cluster stops its motion at a point \vec{s}_2 , as soon as it “touches” the seed located at the origin, or in other terms, once it occupies one of the eight sites closest to the origin.

A third cluster is then dropped onto the substrate at a random starting position – which, again, should not be chosen too far from the two-cluster island already formed. This cluster also diffuses on the surface of the substrate. Its diffusive motion is however biased by an elastic force due to the two-cluster island located around the origin. This force is assumed to derive from the sum $V(\vec{r}) = \alpha \ln(\|\vec{r} - \vec{s}_1\|/r_0) + \alpha \ln(\|\vec{r} - \vec{s}_2\|/r_0)$ of the potentials induced by the first two clusters. The jump probability $p(\vec{r}, \vec{r} + \vec{e}_i)$ is still given by Eq.(4) but now with $\vec{F}(\vec{r}) \equiv -\vec{\nabla}_{\vec{r}}V(\vec{r})$. The biased diffusion stops when the third cluster visits for the first time one of the neighboring sites of the first two aggregated clusters, of position \vec{s}_3 . The general case of the N^{th} deposited cluster follows by analogy.

Note that in this model, the clusters are successively dropped onto the surface, as it is usually assumed in the DLA approach. Though in a real experiment many

clusters diffuse over the surface simultaneously, the interaction among them is negligible as compared to the potential induced by the clusters already aggregated in

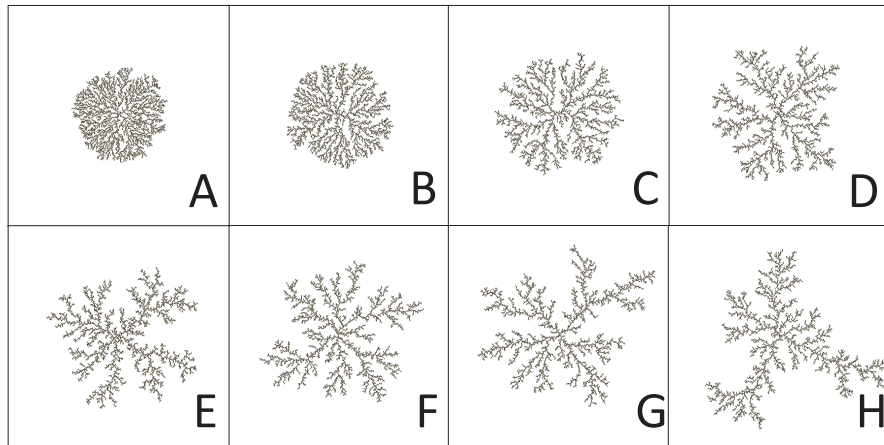


Figure 2: Simulations of our ramified structures obtained in our drifted DLA model by the deposition 6400 clusters for different values of the dimensionless parameter κ : (A) $\kappa = 3,3 \times 10^{-3}$, (B) $\kappa = 1 \times 10^{-3}$, (C) $\kappa = 3,3 \times 10^{-4}$, (D) $\kappa = 1 \times 10^{-4}$, (E) $\kappa = 3,3 \times 10^{-5}$, (F) $\kappa = 0$ corresponding to the standard DLA model, (G) $\kappa = -1 \times 10^{-5}$ and (H) $\kappa = -3,3 \times 10^{-5}$.

a ramified structure. Also note that, in our model, we never make use of any specific property of the interaction mediated by elastic forces. The nature of the interaction might therefore be of a different origin, and the only requirement is that the interaction potential satisfies

$$\Delta V(\vec{r}) = \alpha c(\vec{r}), \quad (5)$$

where $c(\vec{r}) = 1$ for sites occupied by aggregated clusters, and $c(\vec{r}) = 0$ otherwise. As a consequence, it is also possible to make simulations for repulsive potentials, *i.e.* with $\alpha < 0$, which do not correspond to elastic deformations.

In Fig. 2 we present a few simulated pictures obtained through the aggregation of $N = 6400$ clusters whose diffusion was biased by the potential Eq.(5) for different values of the dimensionless parameter $\kappa \equiv \alpha\beta$. As could be expected, for attractive forces $\kappa > 0$ (Fig. 2 A-E), the structures have more compact of the morphologies than those obtained in the DLA model $\kappa = 0$ (Fig. 2 F). In the repulsive regime $\kappa < 0$ (Fig. 2 G,H), the "arms" of the ramified structures, on the contrary tend to repel each other, thus giving rise to less compact structures.

III. CHARACTERIZATION METHOD, DISCUSSION AND RESULTS

The fractal dimension appears as the most natural mathematical tool to characterize ramified structures such as the dendritic islands formed by aggregated atomic clusters, and was intensively used in previous works [6]. There, however, exist different operational definitions of this quantity in the literature which are not equivalent. For instance, the methods based on the radius of gyration

The transition from sparse to compact objects resembles one that has already been observed and modeled in the case of electro-deposition experiments [5, 22], although not for the case of self-consistent interaction but for a fixed external potential.

In Fig. 3 for comparison we show dendritic islands experimentally obtained through depositing (A) silver Ag_{100} [9, 23] and (B) antimony Sb_{500} atomic clusters [10]. At first glance, 3 B (antimony clusters) seem to be well described by the same kind of structures as in Fig. 2 D, corresponding to our drifted DLA model, with a moderate attractive force, whereas 3 A (silver clusters) seem to correspond to none of the structures displayed in Fig. 2, *i.e.* it is satisfactorily described by neither the DLA (Fig. 2 F) nor the drifted DLA models (Fig. 2 A-E,G,H). One, however, needs a more formal tool for quantification of this observation, that would enable one to say how much the simulated structures match the experimental data. In the next section, we introduce such quantities, the regular and the external fractal dimensions. The latter presents the advantage of being particularly sensitive to the elastic force at the core of our model.

[24] or the auto-correlation function [15] as well as multifractal analysis techniques [25] appear very sensitive to the specific features of the structure under consideration. For different DLA simulated morphologies, the fractal dimensions calculated through these methods already show a very large dispersion, typically ranging from 1.67 to 1.72. Because of this dispersion, these methods cannot be expected to precisely distinguish simulations obtained through different types of models.

What we are looking for is, on the contrary, a quan-

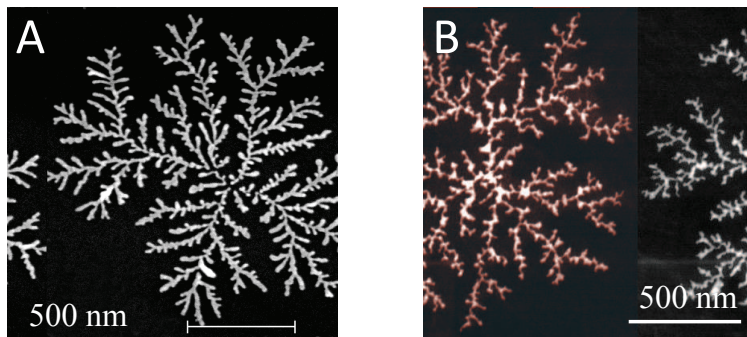


Figure 3: Experimental pictures of single dendrites obtained through the deposition of (A) silver Ag_{100} [9, 23] and (B) antimony Sb_{500} [10] atomic clusters onto graphite HOPG.

tity able to universally characterize all the morphologies simulated by a given model. The fractal dimension D_H calculated according to the Hausdorff-Minkowski definition precisely has this property. As shown in [26], it takes the value $D_H = 1.60$ for any DLA simulated structure with the negligible dispersion ± 0.01 , and we numerically checked the same property for the drifted DLA model. To compute D_H one covers the object with disks of radius r , and measures the area $I_H(r)$ of the object thus formed. The number $N_H(r)$ of these disks is then simply given by $N_H(r) = \frac{I_H(r)}{\pi r^2}$. The fractal dimension D_H is, by definition, determined by the expected asymptotic behaviour $N_H(r) \sim r^{-D_H}$ when $r \rightarrow 0$. Practically, the size of the probe disks should, however, remain larger than the typical size r_c of a cluster in order to avoid spurious and meaningless discretization effects. It must also not be too large, that is, typically, smaller than the radius R of the whole aggregate – when r exceeds R only one disk is necessary to cover the structure and therefore $N_H(r) = 1$. Finally, the quantity $-D_H = \lim_{r \rightarrow 0, r \gg r_c} \frac{\ln N_H(r)}{\ln r}$ appears as the slope of the approximately linear function $\ln N_H(r) = f(\ln r)$ on the intermediate range $[r_c, R]$ (see Fig.4).

The lower curve in Fig. 5 shows the fractal dimension D_H of simulated structures as a function of κ . As expected, the dimension D_H grows with the intensity of the force, which is consistent with the visible increasing compactness of the forms numerically generated. The variations of D_H , however, remain very moderate: quantifying the effects of the elastic field through D_H will therefore not constitute a very sensitive method.

To remedy this problem, we consider an alternative possible characteristic of a ramified fractal-like morphology, the so-called external fractal dimension D_E , which turns out to be much more sensitive to the variations of κ . To our knowledge, this fractal dimension has never been applied in the context of cluster aggregated structures. By definition, D_E is the fractal dimension of the periphery of the object. To be more explicit, one computes D_E by

measuring the area $I_E(r)$ swept by a disk of radius r , sliding along the border of the structure. Intuitively, in a

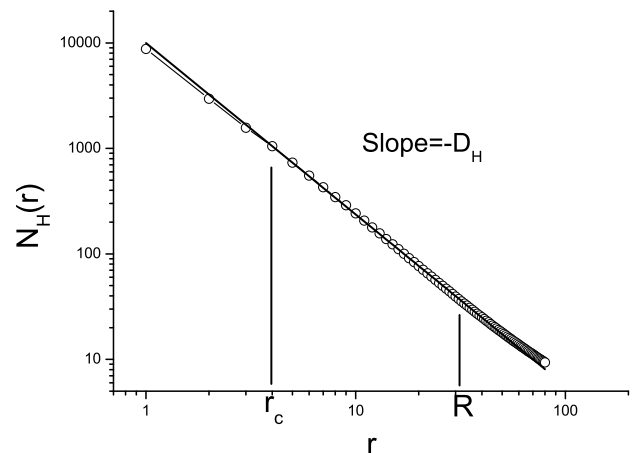


Figure 4: The number of disks $N_H(r)$ covering a ramified simulated structure as a function of the probe disks' radius r , in logarithmic scales. Self-similarity of the fractal-like dendritic structure can be checked on the range $[r_c, R]$.

ramified object, as r decreases, more and more structures appear. This results in a non trivial behaviour of $I_E(r)$, and therefore of $N_E(r) = \frac{I_E(r)}{\pi r^2}$, the number of disks necessary for covering the whole area $I_E(r)$. For a rigorously fractal object $N_E(r) \propto r^{-D_E}$. The same scaling is found in morphologies showing self-similarity on a given range of radii, as the structures generated by our simulations.

The behaviours of D_E and D_H can be compared in the inset of Fig. 5. In particular, it is quite apparent that D_E is much more sensitive to κ than D_H and is therefore a better suited quantity for characterizing the modifications imposed to the aggregated structures by the elastic field.

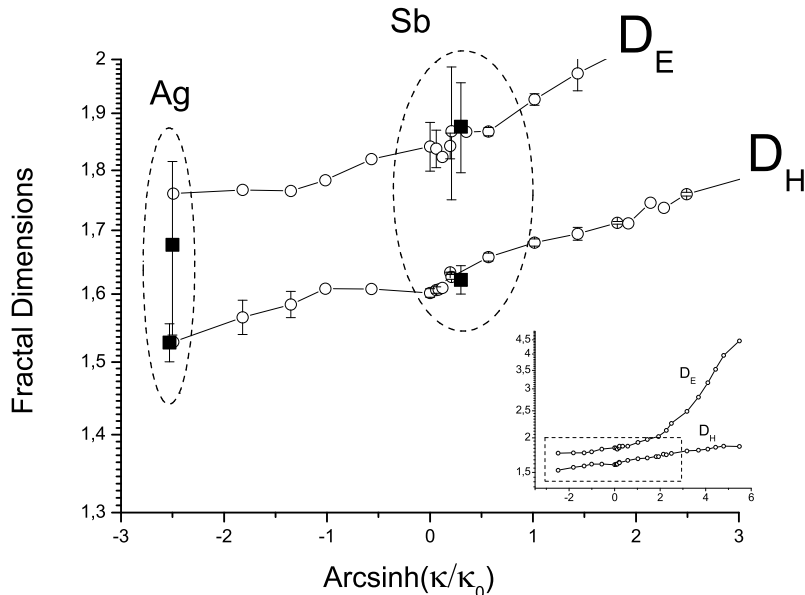


Figure 5: The **inset** presents the behaviours of D_H (lower curve) and D_E (upper curve) of the morphologies obtained by the numerical simulation of our drifted DLA model, as functions of the parameter $\text{arcsinh}(\kappa/\kappa_0)$ characterizing the intensity of the elastic field induced by the growing island ($\kappa_0 = 0.17 \times 10^{-4}$). The **main plot** is a zoom of the inset on the area contained in the dotted box. Two couples of points have been reported, corresponding to the values of D_H and D_E , extracted from a set of experimental pictures obtained by the deposition of silver Ag_{100} [9, 23] and antimony Sb_{500} atomic clusters [10] onto graphite HOPG. The value of the parameter κ is adjusted so as to minimize $|D_H^{\text{th}}(\kappa) - D_H^{\text{exp}}| + |D_E^{\text{th}}(\kappa) - D_E^{\text{exp}}|$ in both cases. The points corresponding to antimony can be reported on the theoretical plot with excellent agreement and correspond to $\kappa_{\text{Sb}} \simeq 5 \times 10^{-6}$ (small attractive potential), while our model seems to fail to correctly describe the experimental values for silver.

IV. COMPARISON WITH EXPERIMENTS

Let us now confront our model to some experimental data available in the literature. We first consider experimental pictures of dendritic structures obtained through depositing Sb_{500} antimony atomic clusters on a graphite HOPG substrate [10], such as Fig. 3 B. Following the same procedures as described above, we extract the Hausdorff and external fractal dimensions of the set of ~ 100 pictures we have, and get the averaged values $D_H^{\text{exp}}(\text{Sb}) \simeq 1.622 \pm 0.022$ and $D_E^{\text{exp}}(\text{Sb}) \simeq 1.876 \pm 0.080$. If our model correctly describes the aggregation of antimony clusters, there must exist a specific value of the parameter κ , denoted by κ_{Sb} , such that drifted-DLA simulations run with this specific parameter κ_{Sb} yield values for D_H and D_E which coincide with the experimental ones. In other terms, there should exist a value κ_{Sb} such that $D_H^{\text{exp}}(\text{Sb}) \simeq D_H^{\text{sim}}(\kappa_{\text{Sb}})$ and $D_E^{\text{exp}}(\text{Sb}) \simeq D_E^{\text{sim}}(\kappa_{\text{Sb}})$ are simultaneously checked – here, $D_{H,E}^{\text{sim}}(\kappa)$ denotes the Hausdorff/external fractal dimension of the structures obtained by drifted-DLA simulations with the parameter κ . To identify such a value, one simply tries to numerically minimize to zero the quantity $|D_H^{\text{sim}}(\kappa) - D_H^{\text{exp}}(\text{Sb})| + |D_E^{\text{sim}}(\kappa) - D_E^{\text{exp}}(\text{Sb})|$. It turns out that the minimization is successful and yields

the value $\kappa_{\text{Sb}} \simeq 5 \times 10^{-6}$. The two experimental values $D_{H,E}^{\text{exp}}(\text{Sb})$ are reported on Fig. 5: the agreement is excellent indeed between model and experiment, which suggests that the physics of aggregation of antimony clusters is actually correctly described by our model and involves a small attractive elastic potential. It is also interesting to note that $\kappa_{\text{Sb}} \simeq 5 \times 10^{-6}$ is precisely the value corresponding to the picture Fig.2D: this means that the experimental picture Fig.3B is indeed better described by a structure of the kind of Fig.2D than by a pure DLA morphology Fig.2F. The visual impression we had at the end of Sec. II is therefore completely confirmed by our quantitative analysis.

We now turn to pictures obtained by depositing Ag_{100} silver atomic clusters [9, 23]. The experimental values we extract are $D_H^{\text{exp}}(\text{Ag}) \simeq 1.528 \pm 0.028$ and $D_E^{\text{exp}}(\text{Ag}) \simeq 1.677 \pm 0.138$. Note that the error bars, especially on $D_E^{\text{exp}}(\text{Ag})$, are too important to make any firm conclusion. This dispersion follows from the small size of the dendrites observed on experimental pictures, which substantially truncates the range $[r_c, R]$ on which self-similarity can be observed. The fractal dimension therefore cannot be extracted with a sufficiently high fidelity. If, however, we apply the same procedure as for antimony, we observe that there exists no value of κ minimizing to zero the quantity

$|D_H^{\text{sim}}(\kappa) - D_H^{\text{exp}}(\text{Ag})| + |D_E^{\text{sim}}(\kappa) - D_E^{\text{exp}}(\text{Ag})|$. The experimental values $D_{H,E}^{\text{exp}}(\text{Ag})$ reported on Fig. 5 correspond to the value $\kappa_{\text{Ag}} \simeq -10^{-4}$ of the parameter κ providing the best compromise, though clearly far from being satisfactory. Note that $\kappa_{\text{Ag}} < 0$ does not correspond to an elastic (attractive) field, the physics of aggregation therefore does not seem governed by the same mechanisms as for Sb. More investigations need be taken to better understand how to account for this specific behaviour.

V. CONCLUSION

We have presented a new class of biased diffusion models for the aggregation of atomic clusters deposited on a plane substrate. This approach can be viewed as a development generalizing the traditionally used DLA model, that we completed by introducing an elastic force originating from the substrate deformation by the growing structure. The diffusion equation which governs the cluster density dynamics is therefore transformed into the Smoluchowski equation. Numerical simulations of our model yield ramified structures, whose compactness is seen to increase with the intensity of the deformation force.

To quantitatively compare the results of our simula-

tions with experimental data, we investigated Hausdorff and external fractal dimensions, and showed that the latter is better suited for characterizing the modifications of the structures obtained in our model due to the elastic field.

Finally, we compared our simulations to already published experimental results, on silver and antimony clusters. Whereas our model describes antimony-cluster-aggregated structures very well, it is not adapted to silver. This suggests that the dynamics of aggregation is dominated by different processes, depending on the atomic nature of the clusters considered. Identifying what these physical processes are, and their exact influence on the form of the morphologies of the corresponding ramified structures is an interesting perspective of the present work. Another possible investigation would consist to apply the same kind of analysis, involving the fractal dimension, to physically completely different domains, such as electro-deposition where DLA approach clearly fails [22].

Acknowledgments

The authors thank F. Prats for fruitful discussions concerning numerical simulations.

-
- [1] R. Tokita, T. Katoh, Y. Maeda, J. Wakita, M. Sano, T. Matsuyama, M. Matsushita, *J. of Phys. Soc. Jap.* **78**, 074005 (2009).
 - [2] L. Niemeyer, L. Pietronero, and H. J. Wiesmann, *Phys. Rev. Lett.* **52**, 1033 (1984).
 - [3] D. Bensimon, L. P. Kadanoff, S. Liang, B. I. Shraiman and C. Tang, *Rev. Mod. Phys.* **58**, 977 (1986).
 - [4] F. Ciuchi, L. Sorriso-Valvo, A. Mazzulla, and J. M. Redondo, *Eur. Phys. J. E* **29**, 139 (2009).
 - [5] T. R. Ní Mhíocháin, G. Hinds, A. Martin, Z. Y. E. Chang, A. Lai, L. Costiner, and J. M. D. Coey, *Elec. Acta* **49**, 4813 (2004).
 - [6] R. Q. Hwang, J. Schröder, C. Günther, and R. J. Behm, *Phys. Rev. Lett.* **67**, 3279 (1991).
 - [7] A. R. Howells, L. Hung, G. S. Chottiner, D. A. Scherson, *Solid State Ionics* **150**, 53 (2002).
 - [8] L. Bardotti, P. Jensen, A. Hoareau, M. Treilleux, and B. Cabaud, *Phys. Rev. Lett.* **74**, 4694 (1995).
 - [9] C. Brechignac et al., *Surf. Sci.* **518**, 192 (2002).
 - [10] B. Yoon et al., *Surf. Sci.* **443**, 76 (1999).
 - [11] L. Bardotti, P. Jensen, A. Hoareau, M. Treilleux, B. Cabaud, A. Perez, F. Cadete Santos Aires, *Surf. Sci.* **367**, 276 (1996).
 - [12] B. B. Mandelbrot, B. Kol, and A. Aharony, *Phys. Rev. Lett.* **88**, 055501 (2002).
 - [13] M. T. Batchelor, C. I. Henry, A. P. Roberts, *Phys. Rev. E* **51**, 807 (1995).
 - [14] B. Schraiman and D. Bensimon, *Phys. Rev. A* **30**, R2840 (1986).
 - [15] T. A. Witten and L. M. Sander, *Phys. Rev. Lett.* **47**, 1400 (1981).
 - [16] L. P. Kadanoff, *J. Stat. Phys.* **39** 267 (1985).
 - [17] M. B. Hastings and L. S. Levitov, *Physica D* **116**, 244 (1998).
 - [18] M. G. Stepanov and L. S. Levitov, *Phys. Rev. E* **63**, 061102 (2001).
 - [19] F. Barra, B. Davidovitch, and I. Procaccia, *Phys Rev E* **65**, 046144 (2002).
 - [20] T. A. Witten and P. Meakin, *Phys. Rev. B* **28**, 5632 (1983).
 - [21] L. D. Landau, E. M. Lifshitz, *Theory of Elasticity*, 3rd edition, Butterworth-Heinemann Ltd (1984).
 - [22] T. R. Ní Mhíocháin and J. M. D. Coey, *Phys. Rev. E* **69**, 061404 (2004).
 - [23] A. Lando, N. Kébaïli, P. Cahuzac, A. Masson, and C. Bréchignac, *Phys. Rev. Lett.* **93**, 133402 (2006).
 - [24] A. Yu. Menshutina, L. N. Shchur, and V. M. Vinokur, *Phys. Rev E* **75**, 010401R (2007).
 - [25] Anton Yu. Menshutina and L. N. Shchur, *Phys. Rev E* **73**, 011407 (2006).
 - [26] W. G. Hanan, D. M. Heffernan, *Chaos, Sol. and Frac.* **12**, 193 (2001).